

Effects of interstitial oxygen on the superconductivity of niobium*

C. C. Koch, J. O. Scarbrough, and D. M. Kroeger

Metals and Ceramics Division, Oak Ridge National Laboratory, Oak Ridge, Tennessee 37830

(Received 14 May 1973)

Superconductivity in niobium-oxygen body-centered-cubic solid-solution alloys (oxygen content 0.024–3.50 at.%) was studied by calorimetric, magnetic, and resistive measurement techniques. These measurements included low-temperature-specific-heat capacity, superconducting-normal transition temperature T_c , direct-current magnetization, and electrical resistivity, as well as x-ray lattice parameter, microhardness, and optical metallography to characterize the samples. Oxygen in solid solution lowers the T_c of niobium. In contrast to the prediction of DeSorbo, we found that γ , the electronic coefficient of low-temperature-specific-heat capacity, also decreases with oxygen concentration. Our data indicated that the “band-structure” electronic density of states at the Fermi level $N_{\text{nb}}(0)$ and the electron-phonon coupling constant λ both decrease with oxygen content. Therefore, both the density of electronic states and the phonon spectrum may be controlling the magnitude of T_c in the niobium-oxygen system. Additional superconducting parameters were calculated for the niobium-oxygen alloys from our calorimetric, magnetic, and resistive data. The Ginzburg-Landau parameter κ_{GL} was found to increase from less than 1.0 for essentially pure Nb to about 10 for the Nb–3.5-at.%-O alloy. Calculated values of $H_{c2}(4.2\text{ K})$ versus atomic-percent oxygen exhibit a maximum at 2-at.% oxygen which was observed experimentally.

I. INTRODUCTION

An understanding of the influence of interstitial elements (O, N, H, C)—particularly oxygen—on the superconducting properties of Nb and its alloys is of interest to both experimentalists and theorists. Oxygen in solid solution in Nb and its alloys, even in the ppm range, can cause marked changes in superconducting properties ranging from fluxoid pinning¹ to the performance of high-frequency accelerator cavities.² Furthermore, to those theorists interested in understanding and predicting the superconducting transition temperature T_c from normal-state parameters, the Nb-O solid solutions present a particularly straightforward system for comparison of experiment with theory.

DeSorbo's work of a decade ago³ remains the most complete study of the influence of interstitial elements on the superconducting properties of niobium. He found that oxygen in interstitial solid solution in bcc Nb markedly reduced the T_c of Nb, almost linearly by 0.93 K per at. % O. Oxygen also increased the normal-state resistivity ρ_n and the superconducting upper critical field H_{c2} . However, DeSorbo calculated from dc magnetization curves that the electronic coefficient of low-temperature-specific-heat capacity γ [and therefore presumably the density of electronic states at the Fermi level $N(0)$] was essentially constant, independent of oxygen content in Nb-O solid solutions. Assuming that γ gives some measure of $N(0)$, this remarkable result indicates that the strong variation of T_c with atomic-percent oxygen is unrelated to the density of states of the alloy. While no general one-to-one relation between T_c and γ [or $N(0)$] has been found (e.g., Ref. 4), such a relation is

at least qualitatively observed for alloys in the central transition metals (4 \leq group No. < 8) (Ref. 5), where the Nb-O alloys occur. Our first interest in the Nb-O system was then to determine γ directly from low-temperature-specific-heat-capacity data in order to examine the above conclusion of DeSorbo. Low-temperature-heat-capacity measurements also provide data for comparison with theories for T_c in terms of normal-state parameters. The most successful theory to date for calculating T_c for strong-coupled transition-metal superconductors is that of McMillan⁶ and its modifications.⁷ McMillan's derivation resulted in the now well-known expression for T_c :

$$T_c = \frac{\langle \omega \rangle}{1.20} \exp\left(\frac{-1.04(1+\lambda)}{\lambda - \mu^*(1+0.62\lambda)}\right), \quad (1)$$

where $\langle \omega \rangle$ is an “average phonon frequency” and has been estimated from the Debye temperature Θ_D so that the preexponential term becomes $\Theta_D/1.45$ (Ref. 6), λ is the electron-phonon coupling constant, and μ^* is the Coulomb pseudopotential which falls in the range ~ 0.1 – 0.15 for most transition metals. This expression was obtained by the numerical solution of the integral equations for the gap parameter using the experimentally determined phonon density of states of Nb. Thus, there should be some confidence in the application of McMillan's formula to Nb-rich dilute solid solutions such as the Nb-O system.

In summary, we have studied the Nb-O solid solutions for the following reasons: (i) to determine γ directly from low-temperature-specific-heat data in order to investigate the conclusion of DeSorbo of the constancy of γ in this system, (ii) to measure the appropriate normal-state param-

eters γ and Θ_D as well as T_c in order to use McMillan's expression to calculate the electron-phonon coupling constant λ and the "band-structure" density of states $N_{bs}(0)$,

$$N_{bs}(0) = N(0)/1 + \lambda, \quad (2)$$

and (iii) to provide a relatively complete set of data on the Nb-O system to aid the investigations of superconducting properties. Thus, in addition to low-temperature heat capacity we have measured T_c , the upper critical field H_{c2} , electrical resistivity ρ_n (at 298 and 4.2 K), x-ray lattice parameter a_0 , diamond-pyramid hardness, and carried out optical-metallography to provide a thorough characterization of the Nb-O samples.

II. EXPERIMENTAL

A. Sample preparation and characterization

Niobium metal in the form of 12.7 and 3-mm-diam rod was obtained from Wah Chang Corp. with the only major metallic impurities Ta (860 ppm) and W (460 ppm). Initial tests were made with 12.7-mm-diam cylinders, but, for convenience in preparing samples for superconducting-property measurements, 3-mm rod samples were subsequently used. The as-received Nb was annealed at 1650 °C for 3 h in a vacuum of 5×10^{-9} torr. The samples—either rods 12.7 mm diam \times 31.8 mm long or bundles of six or seven 3-mm-diam rods 31.8 mm long—were oxidized at 1000 °C in a dynamic pressure of 10^{-5} torr of oxygen. The amount of oxygen introduced was controlled by time at 1000 °C and measured by observing the sample weight change. After oxidation, the samples were heated at 1250 °C in 10^{-9} torr vacuum for about 4 days to homogenize the oxygen concentration. The oxygen contents of the samples determined by weight changes were in good agreement with chemical analyses performed by the Oak Ridge National Laboratory analytical chemistry division. Microhardness measurements were

made on the samples with a diamond-pyramid indenter of a Wolpert-Greiss microhardness tester. Optical metallography was carried out on several of the higher-oxygen-content samples to ensure that the solubility limit had not been exceeded. Conical samples for x-ray diffraction were spark-machined from the sample rods and etched to a point for the Debye-Scherrer technique. The Straumanis method of film loading was employed and precise lattice parameters a_0 were determined to an estimated accuracy of ± 0.0003 Å.

B. Low-temperature measurements

The specific-heat capacities were measured using techniques that have been described previously.⁸ In brief, an adiabatic calorimeter was placed inside a superconducting solenoid capable of producing fields up to 40 kOe. Applied fields of either 20 or 30 kOe were used to suppress the superconductivity. A synthetic addendum (~ 0.1 g) was used consisting of carefully weighed parts (graphite resistance thermometer, manganin wire, and varnish). The addendum heat capacity was established by measurement with a copper-standard specimen and this result was in close agreement with the known specific-heat capacities of the constituent parts. The value was $< 2\%$ of the sample-specific-heat capacities in the temperature range 1–4.5 K. The graphite resistance thermometer was calibrated against the vapor pressure of He⁴ after each cooling to low temperatures and with the magnetic field applied after cooling. The superconducting transition temperatures were determined by a standard inductive method using a doped-Ge resistance thermometer as the temperature sensor.

The upper critical field H_{c2} at 4.2 K, was measured by an automatically recording magnetometer. This magnetometer, after the design of Ward,⁹ is a modification of the ballistic-throw method. The two search coils were positioned in the region of homogeneity ($\pm 1\%$ inside a 76-mm sphere) of a

TABLE I. Experimental results on Nb-O solid solutions.

Alloy at. % O	T_c (K)	γ (mJ/mole K ²)	Θ_D (K)	$\frac{\rho^{298}}{\rho^{4.2}}$	$\rho^{4.2}$ $\mu\Omega$ cm	a_0 (Å) (± 0.0003)	Hardness kg/mm ²	H_{c2} (kOe)
0.024	9.23 \pm 0.01	7.77 \pm 0.05 ^a	256 \pm 3 ^a	151.0	0.098	3.3002	61 \pm 4	2.91
		7.95 \pm 0.05 ^b	278 \pm 7 ^b					
		...	242 \pm 4 ^c					
0.139	9.03 \pm 0.02	7.67 \pm 0.03	256 \pm 2	17.6		3.3000	74 \pm 3	4.15
0.555	8.50 \pm 0.08	7.43 \pm 0.03	260 \pm 2	6.30	2.88	3.3025	134 \pm 3	5.86
0.922	8.10 \pm 0.05	7.23 \pm 0.03	260 \pm 2	4.12		3.3023	177 \pm 4	7.45
1.32	7.85 \pm 0.10	6.92 \pm 0.08	268 \pm 7	3.09		3.3060	222 \pm 4	8.42
2.00	7.33 \pm 0.12	6.67 \pm 0.06	274 \pm 4	2.56	10.0	3.3093	265 \pm 4	9.17
3.50	6.13 \pm 0.13	5.94 \pm 0.02	296 \pm 2	1.86	17.5	3.3130	379 \pm 4	8.51

^aLeast-squares fit to data over 1.4–4.5 K.

^bLeast-squares fit to data over 1.4–3.0 K.

^c Θ_D for temperature range 3.0–4.5 K.

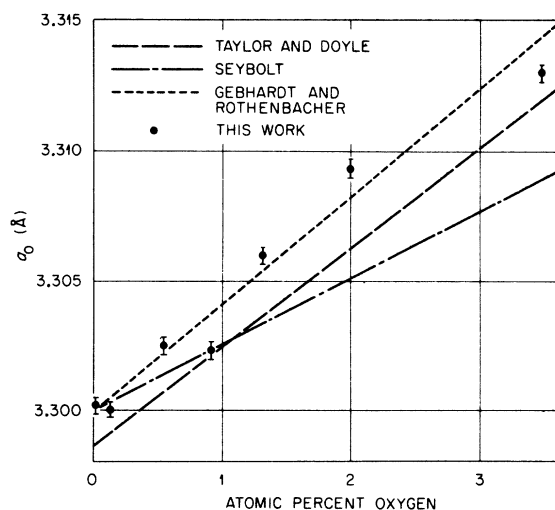


FIG. 1. Lattice parameter a_0 vs atomic-percent oxygen.

superconducting solenoid capable of reaching fields of 72 kOe. The values of H_{c2} were taken directly from the dc magnetization curves.

Electrical resistance measurements were made at room temperature and at 4.2 K using the four-probe technique. The measurements at 4.2 K were made in a magnetic field to suppress the superconductivity.

III. RESULTS

A. Characterization of the Nb-O solid solutions

We first describe the results of measurements made to characterize the Nb-O interstitial solid solutions. All of our experimental measurements are summarized in Table I. The lattice parameters a_0 are plotted against atomic-percent oxygen in Fig. 1 along with curves from the literature.¹⁰⁻¹² There is reasonable agreement with the literature, the closest agreement being with the data of Gebhardt and Rothenbacher.¹¹ A continual increase in a_0 with atomic-percent oxygen is observed.

Microhardness versus atomic-percent oxygen is presented in Fig. 2. The hardness is also a smoothly increasing function of oxygen content and serves as a convenient check on composition.

Electrical resistivity at 4.2 K is plotted against oxygen content in Fig. 3 along with the data of Tedmon *et al.*,¹ limited to low oxygen concentrations, and the data of DeSorbo taken at 10 K.³ DeSorbo's data are essentially parallel to ours, while the resistivity data of Tedmon *et al.* exhibit a higher dependence on oxygen content over the limited range covered. The electrical resistivity ratios $\rho_n^{298\text{ K}}/\rho_n^{4.2\text{ K}}$ for all alloys are listed in Table I.

Optical metallography was carried out on sever-

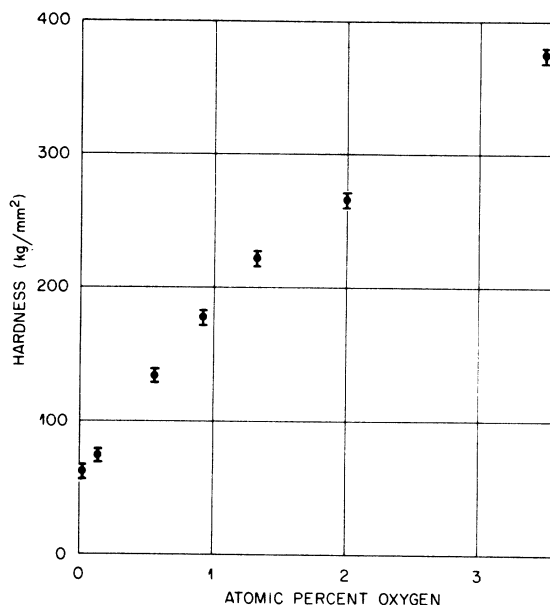


FIG. 2. Hardness vs atomic-percent oxygen.

al samples including the Nb-3.5-at.%-O alloy. Clean equiaxed grains were observed with no indication of precipitation in any of the samples.

The above results all indicate that the solubility limit of oxygen in bcc Nb has not been exceeded. This conforms to the Nb-O phase diagram¹² at our heat treating temperature of 1250 °C, and verifies the efficiency of our quench from this temperature.

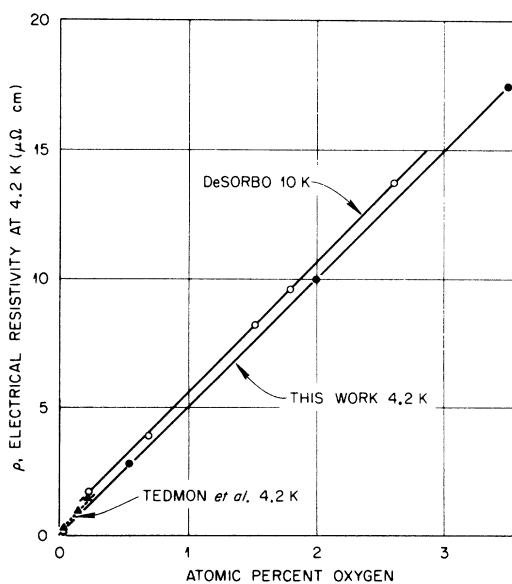


FIG. 3. Electrical resistivity ρ_n at 4.2 K vs atomic-percent oxygen.

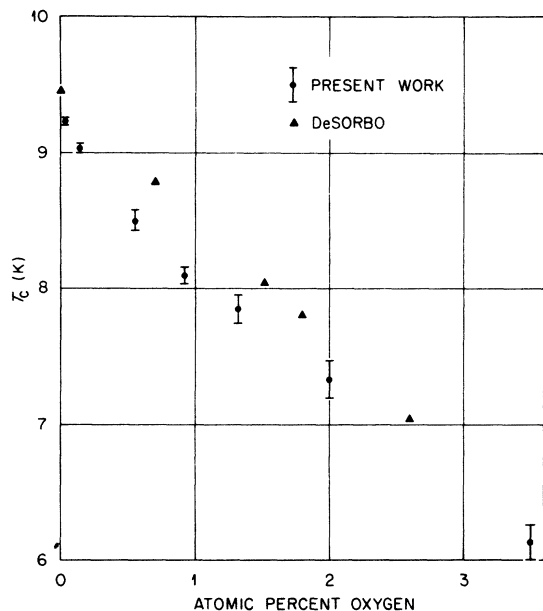


FIG. 4. Superconducting-normal transition temperature T_c vs atomic-percent oxygen.

B. Superconducting measurements

The T_c data are listed in Table I and displayed in Fig. 4 as a function of oxygen content along with DeSorbo's data.³ The bars on our data represent the transition widths, and these relatively sharp transitions give us confidence that the samples were well homogenized regarding oxygen distribution. DeSorbo's T_c data are consistently higher than ours and a line through his experimental

points would be roughly parallel to one through ours. However, his reported T_c for pure Nb (9.46 K) is higher than the usually accepted values for pure Nb (9.2 to 9.3 K).¹³ Since his Nb was reported to be of high purity the discrepancy must stem from measuring technique. If one assumes a similar overestimation of T_c for his other samples, good agreement with the present work is observed.

C. Magnetization measurements H_{c2}

An example of our experimental dc magnetization curves is presented in Fig. 5 for the Nb-2.0-at. % O sample. All the samples showed some hysteresis and the higher-oxygen-content alloys exhibited a small but distinct "peak" in hysteresis near H_{c2} . DeSorbo¹⁴ and others¹⁵ have also observed "peak" effects in critical current density near H_{c2} in Nb-O solid solutions. Figure 5 also shows the weak paramagnetic superconductivity which has been observed in other systems and discussed at length by Hake.¹⁶ The hysteresis present in the magnetization curves facilitated determination of H_{c2} . The H_{c2} values are listed in Table I and plotted in Fig. 6 against oxygen content along with DeSorbo's data for the resistive critical field. Also included in Fig. 6 are curves for calculated H_{c2} values as explained in Sec. IV.

D. Low-temperature-specific-heat-capacity measurements

Low-temperature-specific-heat-capacity data in the form of plots of C/T vs T^2 are presented for selected samples in Fig. 7. Unlike the other Nb-O alloys which exhibit a linear C/T -vs- T^2 plot over the temperature range covered (1-4.5 K),

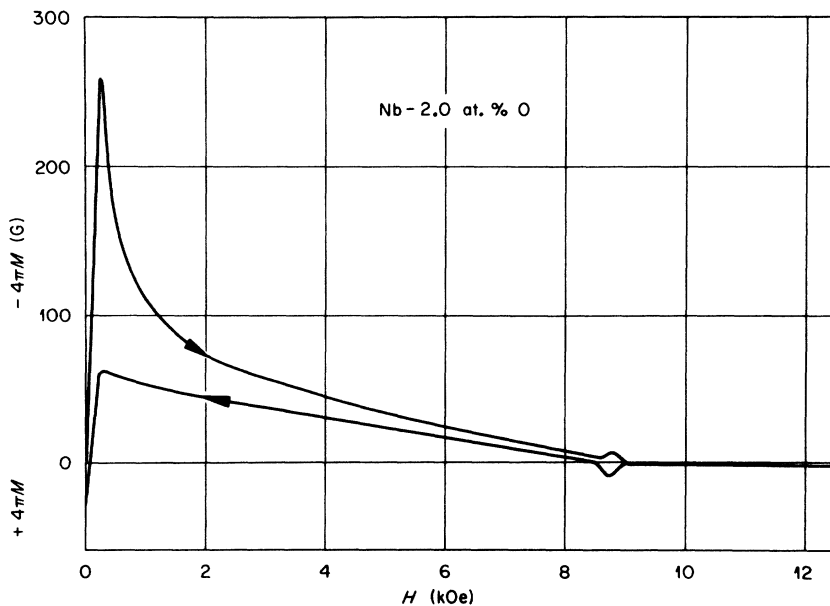


FIG. 5. Magnetization $-4\pi M$ vs H for the Nb-2.0-at. % O alloy.

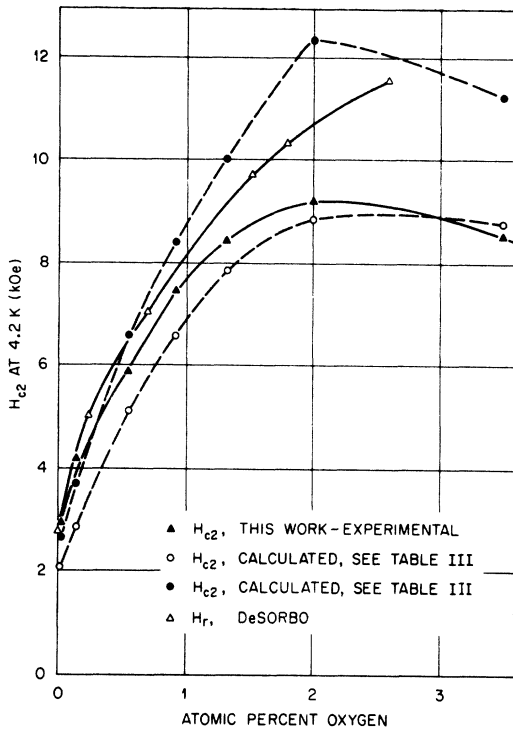


FIG. 6. Upper critical field H_{c2} at 4.2 K vs atomic-percent oxygen. (\blacktriangle — \blacktriangle this work, experimental; \circ — \circ calculated with $\kappa_1(0)/\kappa_{GL}=1.2$; \bullet — \bullet calculated with $\kappa_1(0)/\kappa_{GL}=1.54$; \triangle — \triangle DeSorbo (Ref. 3) resistive critical field H_r .)

the Nb-0.024-at.-%-O samples's ("pure Nb") C/T -vs- T^2 plot shows a definite curvature which can be interpreted as two linear segments which join at $T^2 \approx 9$. Such curvature in C/T vs T^2 has been observed in nominally pure Nb by a number of investigators.^{4,17-19} It has been rationalized as a change in the phonon spectrum of the metal with temperature; that is, the Debye temperature gradually decreases with temperature. This complicates our calculations and correlations with the other Nb-O samples which do not show the above "anomalous" specific-heat behavior. However, we have extracted values of γ and Θ_D from least-squares fits of (i) all the data (ignoring the curvature), (ii) the data for temperatures < 3.0 K, and (iii) the data for temperatures > 3.0 K. The Θ_D , 278 K, from the $T < 3.0$ -K region agrees with the literature values,¹⁷⁻¹⁹ while the γ , 7.95 ± 0.05 mJ/mole K², from this region is slightly higher. The values of Θ_D and γ extracted from all the data are also in reasonable agreement with the results of those previous workers (e.g., Ref. 20) who did not observe or ignore the curvature in the C/T -vs- T^2 plot. In any event, it is evident from Fig. 7 that the addition of oxygen to niobium decreases γ (the

C/T -axis intercept) and increases Θ_D [$\Theta_D = (12\pi^4 R / 5\beta)^{1/3}$, where β is the slope of the C/T -vs- T^2 curve and R is the gas constant]. The values of γ and Θ_D are plotted explicitly against atomic-percent oxygen in Figs. 8 and 9, respectively. In these figures (and Table I) the Θ_D and γ for Nb-0.024-at.-%O are plotted for the region < 3.0 K and for the entire temperature range. While there is little choice between the two γ values for Nb-0.024-at.-%O in terms of a reasonable trend in Fig. 8 it is apparent that the Θ_D value obtained from the data below 3.0 K does not fit the curve of Fig. 9 nearly so well as the Θ_D obtained using all the data.

IV. DISCUSSION

Contrary to the conclusions of DeSorbo, who indicated γ should be approximately constant in Nb-O solid solutions, we found γ , determined from low-temperature-specific-heat-capacity measurements, to decrease markedly with oxygen concentration, as Fig. 8 illustrates. DeSorbo calculated γ from his magnetization data from the following two expressions:

$$\gamma = 0.17H_c(0)^2/T_c^2, \quad (3)$$

$$\gamma = \frac{V}{8\pi} \left(\frac{\partial H_c}{\partial T} \right)_{T=T_c}^2. \quad (4)$$

His calculations of γ from these formulas are plotted along with our experimental results against oxygen concentration in Fig. 10. DeSorbo made several assumptions and approximations in his calculations which apparently were not justified. First of all he calculated H_c from the area under the magnetization curve in increasing field only. Since the magnetization curves were not fully reversible this could be the source of considerable error. The calculation of γ from Eq. (3), which is the BCS law of corresponding states, gives qualitative agreement with our experimental values, but a weaker dependence of γ on percent oxygen and consistently higher γ values. Since DeSorbo's T_c values were higher than ours and his values of $H_c(0)$ (at least for pure Nb) were slightly underestimated one cannot explain the calculated γ values from his data alone but rather one must conclude the BCS expression is not adequate for accurately calculating γ in strong-coupled transition-metal superconductors such as Nb and the Nb-O alloys. Equation (4) does not even give the correct qualitative dependence on percent oxygen from his data. However, the quantity $(\partial H_c / \partial T)_{T=T_c}^2$ was obtained for H_c data taken near ~ 4.2 K and then fit to

$$H_c = H_c(0)(1 - t^2) \quad (5)$$

to obtain the entire H_c -vs- T curve. Using data at $t \sim 0.45$ – 0.60 to extrapolate $\partial H_c / \partial T$ at $t = 1$ was

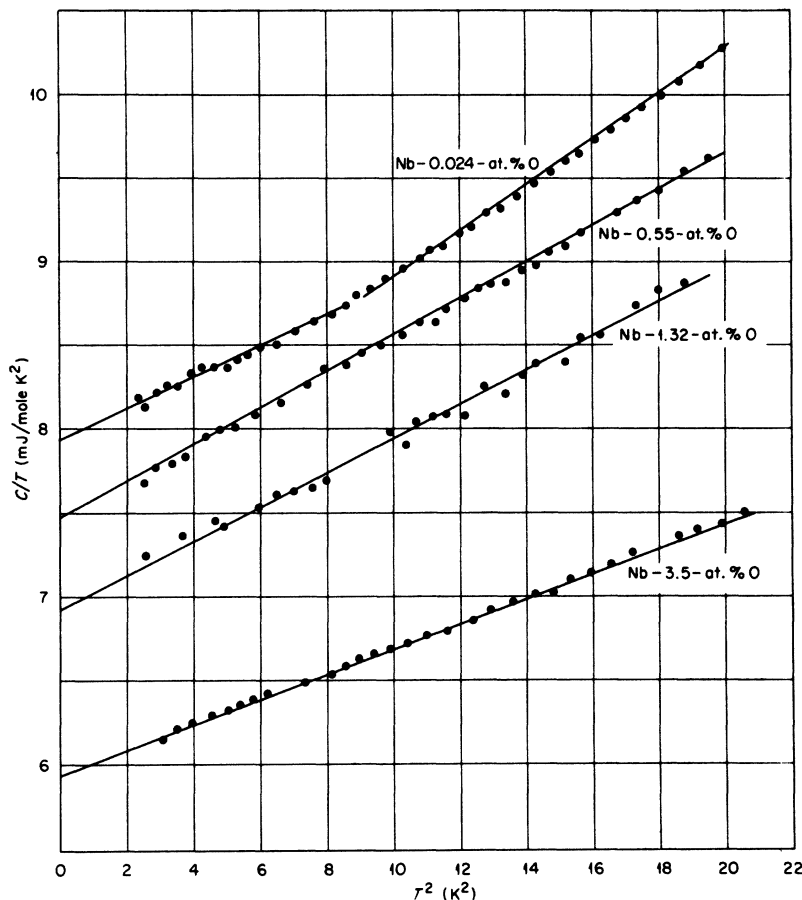


FIG. 7. C/T vs T^2 for selected Nb-O alloys.

apparently not a valid procedure. Thus, the conclusions of DeSorbo regarding the essential constancy of γ in the Nb-O system are not valid since γ decreases with oxygen concentration as observed in the present work, and as indeed he calculated from Eq. (3) for his magnetization data.

With our calorimetric data on the Nb-O system we are able to calculate the electron-phonon coupling constant, λ , from McMillan's analysis.⁶ That is,

$$\lambda = \frac{1.04 + \mu^* \ln(\Theta_D/1.45T_c)}{(1 - 0.62\mu^*) \ln(\Theta_D/1.45T_c) - 1.04}. \quad (6)$$

We have assumed μ^* to be essentially constant and equal to the value 0.15 which was calculated for pure Nb by Bennemann and Garland.²¹ We then have used our experimentally determined values of T_c and Θ_D to calculate λ , and the results are listed in Table II and plotted against atomic-percent oxygen in Fig. 11. There is a question as to which Θ_D one would choose to use in McMillan's expression for the Nb-0.024-at.%-O sample since there are several possibilities (i. e., $\Theta_D = 278$ K, $T < 3$ K; $\Theta_D = 256$ K, $T < 4.5$ K; $\Theta_D = 242$ K, $T > 3$ K). Bennemann and Garland²¹ present a value $\lambda = 0.92$

for pure Nb which they calculated using experimental phonon density-of-states data, i. e., no approximation involving Θ_D . If we use this value of λ for Nb-0.024-at.% O, we can back-calculate and obtain a $\Theta_D = 248$ K which is closer to the values we obtain on ignoring the break in the C/T -vs T^2 curve at ~ 3.0 K. The use of the $\Theta_D = 278$ K (from $T < 3$ -K data) results in a $\lambda = 0.875$ which does not fit the other data smoothly. Of course, the use of Θ_D for calculating λ is only an approximation which assumes Θ_D scales with $\langle \omega \rangle$, the appropriate average phonon frequency. Dynes²² has recently pointed out that the McMillan equation is remarkably accurate if $\langle \omega \rangle$ is used, but that the use of Θ_D is indeed only an approximation which may not be valid in many cases. However, the above calculations for λ should be at least qualitatively correct and these values indicate that oxygen dramatically and steadily decreases the electron-phonon coupling constant of Nb.

With our experimental values for γ and our values calculated for λ we can then calculate the "band-structure" density-of-states $N_{bs}(0)$ from the relationship

$$N_{bs}(0) = 3\gamma/2\pi^2 k_B^2 (1 + \lambda) \quad (7)$$

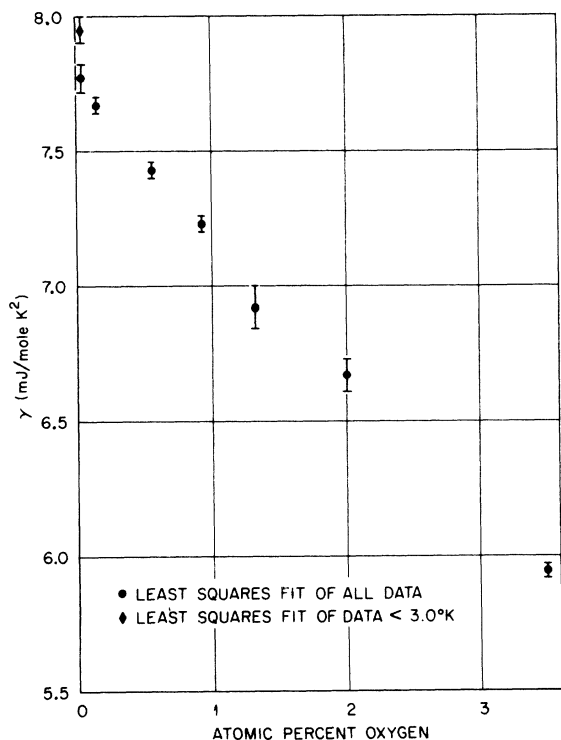


FIG. 8. Electronic coefficient of low-temperature-specific-heat capacity γ vs atomic-percent oxygen.

where k_B is Boltzmann's constant. This is the free-electron density of states modified by the electron-phonon enhancement factor $(1 + \lambda)$ and has been found to agree reasonably well with first-principle band-structure calculations.^{6,23} The values of $N_{bs}(0)$ are listed in Table II and plotted versus atomic-percent oxygen in Fig. 12. Again two values for the Nb-0.024-at.-%-O alloy are possible and are plotted. It is evident that the addition of oxygen monotonically decreases the value of $N_{bs}(0)$ for Nb. Since both $N_{bs}(0)$ and λ decrease with oxygen concentration in Nb it is not possible to separate the effects of electronic density of states [$N_{bs}(0)$] and lattice stiffness (λ) on T_c in these alloys. [λ is primarily governed by the phonon factor $M\langle\omega^2\rangle$ (M = atomic mass) or lattice stiffness, in those bcc transition metals for which suitable data exist.⁶]

The T_c of Nb has also been lowered by preparing Nb in the form of thin amorphous films deposited at low temperatures.^{24,25} The reduction of T_c in this case has been rationalized as a "disorder" effect²⁴ in that the small (~ 10 Å) electron mean free path in these films causes a smearing of the structure in $N(0)$. For Nb which is situated on a peak in $N(0)$ this results in a lower $N(0)$ and thus lower T_c . These thin film results have been

thought²⁵ to reflect the control of T_c across the Periodic Table by an "atomic parameter" after $N(0)$ has been smoothed out by the disorder. It is unlikely that oxygen in our bulk crystalline samples is changing T_c by a similar disorder effect. The electron mean free path calculated from ρ_n for our most concentrated alloy (3.5-at.-% oxygen) is on the order of 100 Å, 10 times larger than for amorphous Nb films with a similar T_c .²⁴ Also, other interstitial elements in Nb such as nitrogen³ cause a smaller effect on T_c than oxygen for the same change in ρ_n . Therefore, oxygen is producing an "alloying" effect and not simply reducing the electron mean free path of Nb.

We are able to calculate and compare several parameters in the theory of type-II superconductors from our calorimetric and magnetization data. First we calculate $H_c(0)$, the thermodynamic critical field at $T=0$, from the relation²⁶

$$H_c(0) = 2.44\gamma^{1/2}T_c, \quad (8)$$

where γ is in $\text{erg}/\text{cm}^3\text{K}^2$. The units conversion was done by using the molar volume calculated from our experimental lattice parameters. The values for $H_c(0)$ as well as the following parameters are listed in Table III. We then assume the relationship

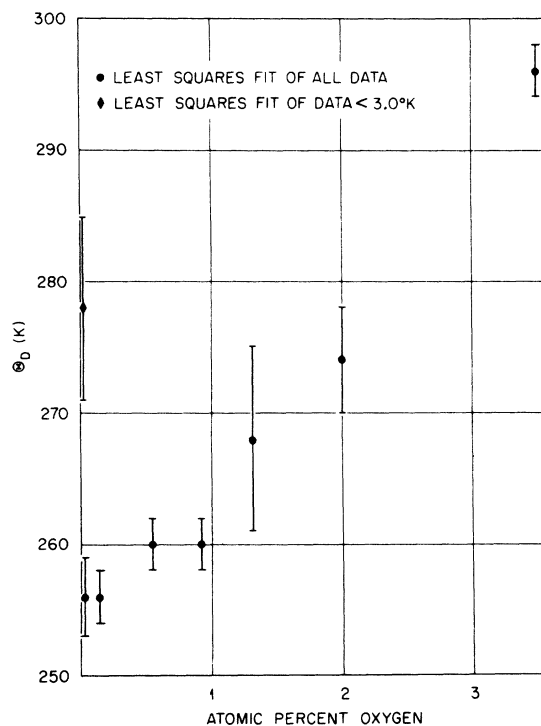


FIG. 9. Debye temperature Θ_D vs atomic-percent oxygen.

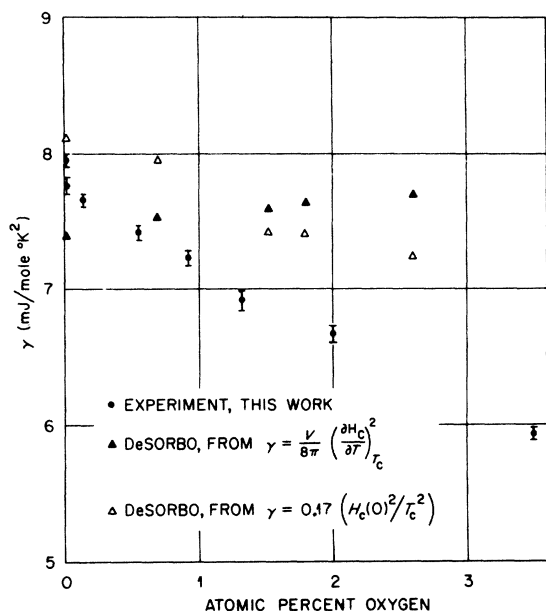


FIG. 10. Electronic coefficient of low-temperature-specific-heat capacity γ vs atomic-percent oxygen. Comparison of DeSorbo's (Ref. 3) calculated γ values with our experimental values.

$$H_c(t) = H_c(0)(1 - t^2) \quad (9)$$

in order to calculate H_c at 4.2 K, where $t = (4.2 \text{ K})/T_c$. The value $H_c(4.2 \text{ K}) = 1515 \text{ Oe}$ for the Nb-0.024-at. % O alloy can be compared to 1584 Oe for high-purity Nb from the magnetization data of Finnemore *et al.*²⁷ We may then calculate the general Ginzburg-Landau parameter κ_1 , introduced by Maki,²⁸ from the expression

$$\kappa_1 = H_{c2}(t)/(2)^{1/2}H_c(t), \quad (10)$$

our experimental values for $H_{c2}(t)$, and the calculated $H_c(t)$ values. We can then estimate the Ginzburg-Landau parameter κ_{GL} from the temperature

TABLE II. Calculated values for λ , $N(0)$, and $N_{bs}(0)$ for Nb-O solid solutions.

Alloy (at. % O)	λ	$N(0)$ (states/eV atom)	$N_{bs}(0)$ (states/eV atom)
0.024	0.92 ^a	1.69 ^b	0.878 ^b
	0.875 ^b	1.65 ^c	0.858 ^c
	0.906 ^c		
0.139	0.897	1.63	0.859
0.555	0.868	1.58	0.846
0.922	0.851	1.53	0.827
1.32	0.829	1.47	0.804
2.00	0.801	1.41	0.783
3.50	0.732	1.26	0.727

^aBennemann and Garland for pure Nb²¹.

^bFrom <3.0-K data.

^cFrom all data.

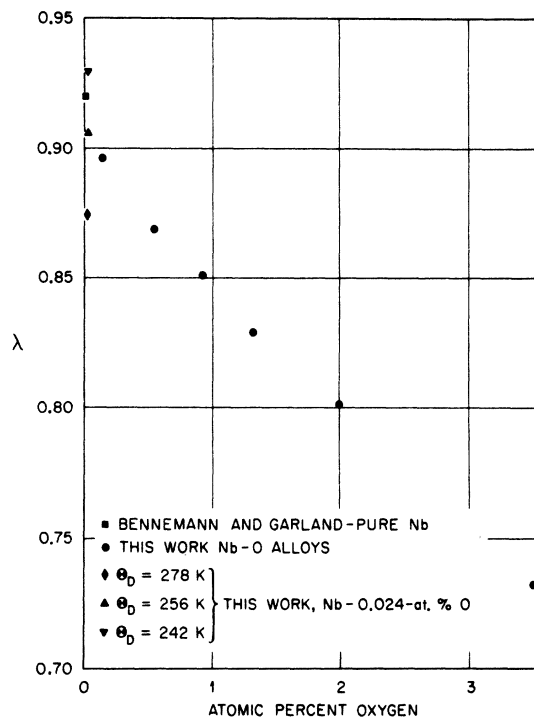


FIG. 11. Electron-phonon coupling constant λ vs atomic-percent oxygen.

dependence of κ_1/κ_{GL} presented by Serin²⁹ who used the data of Finnemore *et al.*²⁷ for pure Nb. We can also estimate κ_{GL} from the Goodman relationship³⁰

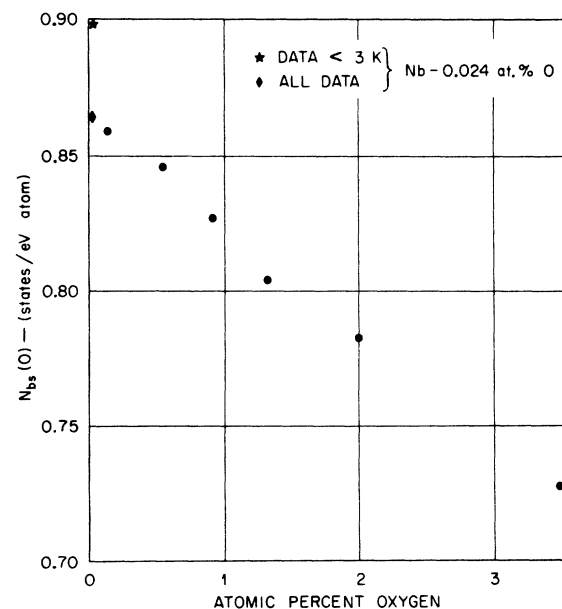


FIG. 12. "Band-structure" density of states $N_{bs}(0)$ vs atomic-percent oxygen.

TABLE III. Some superconducting parameters for the Nb-O solid solutions.

Alloy (at. % O)	$H_c(0)$ (Oe)	$H_c(4.2 \text{ K})$ (Oe)	κ_1 (4.2 K)	κ_{GL}^a	κ_{GL}^b	With $\kappa_1(0) = 1.54\kappa_{GL}$		With $\kappa_1(0) = 1.2\kappa_{GL}$	
						$H_{c2}(0)$ (kOe)	$H_{c2}(4.2 \text{ K})$ (kOe)	$H_{c2}(0)$ (kOe)	$H_{c2}(4.2 \text{ K})$ (kOe)
0.024	1910	1515	1.36	0.98	0.84	3.51	2.64	2.74	2.06
0.139	1854	1453	2.02	1.47	1.22	4.94	3.66	3.85	2.85
0.555	1717	1298	3.19	2.36	2.57	9.43	6.56	7.35	5.11
0.922	1613	1179	4.47	3.37	3.60	12.6	8.42	9.86	6.57
1.32	1528	1091	5.46	4.16	4.73	15.8	10.0	12.3	7.83
2.00	1399	940	6.90	5.39	6.65	20.3	12.3	14.6	8.85
3.50	1102	585	10.3	8.71	10.4	25.1	11.2	19.6	8.75

^a κ_{GL} from κ_1/κ_{GL} at 4.2 K from Serin (Ref. 27) using data of Finnemore *et al.* (Ref. 25).

^b κ_{GL} from $\kappa_{GL} = \kappa_0 + 7.5 \times 10^{-3} \rho_n \gamma^{1/2}$, where κ_0 is assumed to be 0.78 [Finnemore *et al.* (Ref. 25)].

$$\kappa_{GL} = \kappa_0 + 7.5 \times 10^{-3} \rho_n \gamma^{1/2}, \quad (11)$$

where κ_0 is κ_{GL} for the pure solvent (Nb). We have used the value $\kappa_0 = 0.78$ for pure Nb from the data of Finnemore *et al.*²⁷ and our experimental values of ρ_n and γ . The κ_{GL} values calculated by these two methods from our experimental data agree to within 20% or better. Both methods involve approximations. The calculation of $H_c(0)$ from the BCS formula is not strictly applicable to Nb and Nb-O alloys. The temperature dependence of κ_1/κ_{GL} was taken from the experimental data for high-purity Nb²⁷ and may not be the same for the Nb-O alloys. It is not the same as the κ_1/κ_{GL} dependence predicted theoretically for either the "clean" or "dirty" limits.³¹ The Goodman relationship was derived from the Gorkov relation connecting κ_{GL} with mean free path and should be valid in the Ginzburg-Landau regime—i. e., near T_c . We have used $\kappa_0 = 0.78$ which was obtained from the Maki parameters κ_1 and κ_2 at $\sim T_c$ by Finnemore *et al.*²⁷ on pure Nb. Since there are fewer approximations and assumptions involved in calculating κ_{GL} by the Goodman relation we feel the values obtained by this method are more reliable than those obtained by the other method described above.

We may also calculate $H_{c2}(0)$ and $H_{c2}(4.2 \text{ K})$ from our γ , T_c , and ρ_n data. We combine Eq. (11) with Eqs. (10) and (8), and two assumptions for $\kappa_1(0)/\kappa_{GL}$. We obtain the expression

$$H_{c2}(0) = A(2.44\gamma^{1/2}T_c\kappa_0 + 1.83 \times 10^{-2}\gamma T_c\rho_n), \quad (12)$$

where $A = 2.18$ if we assume $\kappa_1(0)/\kappa_{GL} = 1.54$ from the data of Finnemore *et al.*²⁷ on pure Nb, or $A = 1.70$ if we assume the theoretical prediction $\kappa_1(0)/\kappa_{GL} = 1.20$ for the "dirty" limit.³¹ We then

calculate $H_{c2}(4.2 \text{ K})$ from $H_{c2}(0)$ from the theory of Helfand and Werthamer³¹ for the dirty limit and in the absence of paramagnetic effects. The two calculated curves of $H_{c2}(4.2 \text{ K})$ versus atomic-percent oxygen are compared with the experimental curve for $H_{c2}(4.2 \text{ K})$ in Fig. 6. There is fair agreement between calculated and experimental values at low oxygen contents using the $\kappa_1(0)/\kappa_{GL} = 1.54$ derived for pure Nb but in higher oxygen alloys H_{c2} is overestimated. Conversely, using the theoretical $\kappa_1(0)/\kappa_{GL} = 1.2$ ("dirty" limit) gives better agreement with calculated and experimental H_{c2} values at high oxygen contents. Both calculations predict the maximum in $H_{c2}(4.2 \text{ K})$ at Nb-2.0-at. % O, which is observed experimentally.

V. SUMMARY AND CONCLUSIONS

Oxygen in solid solution in niobium dramatically lowers T_c . Our measurements indicate both γ [therefore $N(0)$] and λ decrease with oxygen in niobium so it is not possible to say whether the density of electronic states or the phonon spectrum is more important in controlling T_c in this system.

We were able to calculate several of the important superconducting parameters of the Nb-O alloys from our calorimetric, magnetic, and resistive measurements. The Ginzburg-Landau parameter κ_{GL} was found to increase from less than 1.0 for approximately pure niobium to about 10.0 for the Nb-3.5-at. % O alloy. Calculated values of $H_{c2}(4.2 \text{ K})$ predicted the maximum in H_{c2} at 2-at. % O which was observed experimentally.

ACKNOWLEDGMENTS

The authors wish to thank W. A. Coghlan, T. G. Kollie, and C. J. McHargue for useful comments on the manuscript.

*Research sponsored by the U. S. Atomic Energy Commission under contract with the Union Carbide Corp.

¹C. S. Tedmon, R. M. Rose, and J. Wulff, J. Appl.

Phys. **36**, 164 (1965).

²M. Strongin, H. H. Farrell, C. Varmazis, H. J. Halama, O. F. Kammerer, M. N. Varma, and J. M.

- Dickey, *Proceedings of 1972 Applied Superconductivity Conference, May, 1972* (IEEE, New York, 1972) p. 667.
- ³W. DeSorbo, *Phys. Rev.* **132**, 107 (1963).
- ⁴M. Ishikawa and L. E. Toth, *Phys. Rev. B* **3**, 1856 (1971).
- ⁵G. Gladstone, M. A. Jensen, and J. R. Schrieffer, in *Superconductivity*, edited by R. D. Parks (Marcel Dekker, New York, 1969), Vol. II, p. 740.
- ⁶W. L. McMillan, *Phys. Rev.* **167**, 331 (1968).
- ⁷J. W. Garland and P. B. Allen, in *Proceedings of the International Conference on the Science of Superconductivity, Stanford, California, 1969*, edited by F. Chilton (North-Holland, Amsterdam, 1971), p. 669.
- ⁸G. D. Kneip, J. O. Betterton, and J. O. Scarbrough, *Phys. Rev.* **130**, 1687 (1963).
- ⁹D. Ward, *Cryogenics* **7**, 41 (1967).
- ¹⁰A. U. Seybolt, *Trans. AIME* **200**, 770 (1954).
- ¹¹E. Gebhardt and R. Rothenbacher, *Z. Metallk.* **54**, 443 (1963); *Z. Metallk.* **54**, 623 (1963).
- ¹²A. Taylor and N. J. Doyle, *J. Less Common Metals* **13**, 313 (1967).
- ¹³B. W. Roberts, *Superconductive Materials and Some of Their Properties*, NBS Tech. Note No. 482 (U. S. GPO, Washington, D. C., 1969), VIII-59.
- ¹⁴W. DeSorbo, *Phys. Rev.* **134**, A1119 (1964); *Rev. Mod. Phys.* **36**, 90 (1964).
- ¹⁵K. A. Jones and R. M. Rose, *Trans. AIME* **245**, 67 (1969).
- ¹⁶R. R. Hake, *Phys. Rev.* **158**, 356 (1967).
- ¹⁷B. J. C. Van der Hoeven, Jr. and P. H. Keesom, *Phys. Rev.* **134**, A1320 (1964).
- ¹⁸H. A. Leupold and H. A. Boorse, *Phys. Rev.* **134**, A1322 (1964).
- ¹⁹L. Yun Lung Shen, N. M. Senozan, and N. E. Phillips, *Phys. Rev. Lett.* **14**, 1025 (1965).
- ²⁰J. M. Corsan and A. J. Cook, *Phys. Status Solidi* **40**, 657 (1970).
- ²¹K. H. Bennemann and J. W. Garland, *AIP Conf. Proc.* **4**, 116 (1972).
- ²²R. C. Dynes, *Solid State Commun.* **10**, 615 (1972).
- ²³L. F. Mattheiss, *Phys. Rev. B* **1**, 373 (1970).
- ²⁴J. E. Crow, M. Strongin, R. S. Thompson, and O. F. Kammerer, *Phys. Lett. A* **30**, 161 (1969).
- ²⁵M. M. Collver and R. H. Hammond, *Phys. Rev. Lett.* **30**, 92 (1973).
- ²⁶J. Bardeen, L. N. Cooper, and J. R. Schrieffer, *Phys. Rev.* **108**, 1175 (1957).
- ²⁷D. K. Finnemore, T. F. Stromberg, and C. A. Swenson, *Phys. Rev.* **149**, 231 (1966).
- ²⁸K. Maki, *Physics* **1**, 21 (1964); 127 (1964).
- ²⁹B. Serin, in Ref. 5, p. 940.
- ³⁰B. B. Goodman, *IBM J. Res. Dev.* **6**, 63 (1962).
- ³¹E. Helfand and N. R. Werthamer, *Phys. Rev.* **147**, 288 (1966).